Title
Application of a detailed dimensional solid oxide fuel cell model in integrated gasification fuel cell system design and analysis

Journal
Journal of Power Sources, 196(14)

ISSN
0378-7753

Authors
Li, Mu
Brouwer, Jacob
Rao, Ashok D
et al.

Publication Date
2011-07-01

DOI
10.1016/j.jpowsour.2011.02.080

Journal of Power Sources 196 (2011) 5903–5912

Contents lists available at ScienceDirect

Journal of Power Sources

journal homepage: www.elsevier.com/locate/jpowsour

Application of a detailed dimensional solid oxide fuel cell model in integrated gasification fuel cell system design and analysis

Mu Li, Jacob Brouwer*, Ashok D. Rao, G. Scott Samuelsen

Advanced Power and Energy Program, University of California, Irvine, CA 92697-3550, USA

ARTICLE INFO

Article history:
Received 5 January 2011
Received in revised form 24 February 2011
Accepted 28 February 2011
Available online 5 March 2011

Keywords:
SOFC
IGFC
CO_2 Capture
SOFC modeling

ABSTRACT

Integrated gasification fuel cell (IGFC) systems that combine coal gasification and solid oxide fuel cells (SOFC) are promising for highly efficient and environmentally sensitive utilization of coal for power production. Most IGFC system analysis efforts performed to-date have employed non-dimensional SOFC models, which predict SOFC performance based upon global mass and energy balances that do not resolve important intrinsic constraints of SOFC operation, such as the limits of internal temperatures and species concentrations. In this work, a detailed dimensional planar SOFC model is applied in IGFC system analysis to investigate these constraints and their implications and effects on the system performance. The analysis results further confirm the need for employing a dimensional SOFC model in IGFC system design. To maintain the SOFC internal temperature within a safe operating range, the required cooling air flow rate is much larger than that predicted by the non-dimensional SOFC model, which results in a larger air compressor design and operating power that significantly reduces the system efficiency. Options to mitigate the challenges introduced by considering the intrinsic constraints of SOFC operation in the analyses and improve IGFC design and operation have also been investigated. Novel design concepts that include staged SOFC stacks and cascading air flow can achieve a system efficiency that is close to that of the baseline analyses, which did not consider the intrinsic SOFC limitations.

1. Introduction

Coal-based power plants with low criteria pollutant emissions and carbon capture capability are essential for satisfying the ever increasing global energy demand while protecting the earth from pollution and climate change. Conceptual design and analyses of the integration of coal gasifiers with high temperature fuel cells have attracted much research interest around the world since the early 1990s and the results have clearly shown the potential of such systems for superior efficiency and emissions compared to other system approaches, including integrated gasification combined cycle (IGCC) systems [1–10]. Recently, IGFC systems that take advantage of more efficient catalytic gasifiers and the cooling caused by direct internal reforming (DIR) of CH_4 to reduce parasitic air compression load, have been proposed [11,12] and the electrical efficiency of such systems have been estimated to exceed or approach the U.S. Department of Energy (DOE) performance goal for next generation coal-based power plants: producing electricity at 60% efficiency (coal HHV basis) while capturing more than 90% of the inlet fuel carbon in a pure CO_2 stream [13].

However, the system performance of these designs needs further scrutinization because most of the published efforts are based upon use of non-dimensional SOFC models that only analyze the global mass and energy balances of the SOFC. As an electrochemical energy conversion device, the performance and safe operation of SOFC are also significantly affected by the internal distributions of temperature and species concentrations, which are beyond the resolution capability of non-dimensional SOFC models. To clarify this issue, a detailed dimensional model for planar SOFC has been previously developed for use in such IGFC system analysis work [14]. The current work demonstrates and discusses the application of this model to the design and analysis of IGFC systems.

To provide a system level background to carry on the discussions, an IGFC system consisting of catalytic hydro-gasification and hybrid pressurized SOFC – gas turbine power block, which is one of the most promising system configurations obtained in previous non-dimensional SOFC model based design and analysis [12], has been chosen as a "baseline" case in this work. The detailed dimensional SOFC model is introduced in the place of the previously used non-dimensional SOFC model and the system design criteria and configurations are modified accordingly to accommodate the new constraints. Differences in system design approaches and system performance are investigated and presented.

* Corresponding author. Tel.: +1 949 824 1999; fax: +1 949 824 7423.
E-mail address: jb@nfcrc.uci.edu (J. Brouwer).

0378-7753/$ – see front matter © 2011 Elsevier B.V. All rights reserved.
doi:10.1016/j.jpowsour.2011.02.080

Nomenclature

A	area, m^2
$D_{i,eff}$	effective diffusivity of species i in porous materials, $m^2\ s^{-1}$
E^0	ideal potential of H_2 oxidization at ambient pressure
E_{act}	activation energy, $kJ\ mol^{-1}$
K	convective heat transfer coefficient, $W\ m^{-2}\ K^{-1}$
K_p	equilibrium constant
R	ohmic resistance, Ω or: heat conduction resistance, $W\ K^{-1}$
T	temperature, K
V	voltage, V
h	specific enthalpy of species, $J\ mol^{-1}$
i	electric current, A
j	electric current density, $A\ m^{-2}$
j_0	exchange current density, $A\ m^{-2}$
p	pressure, bar
r	rate of reaction, $mol\ s^{-1}$
x_i	molar fraction of species i
α	electron transfer coefficient
γ	pre-exponential factor in exchange current density calculation
δ	thickness, m

Subscript

IC	interconnect
PEN	positive-electrolyte-negative structure
air	air or air side
amb	ambient conditions
an	anode
cat	cathode
ele	electrolyte or related to electrochemical oxidation of H_2
fuel	fuel or fuel side
rx	methane reforming reaction
shift	water gas shift reaction

Superscript

an	anode
b	bulk flow
cat	cathode
r	reaction site

2. The dimensional SOFC model

Many models have been developed to provide detailed insights into SOFC operation [15–18]. The model used in this work is a quasi-two-dimensional finite volume model for planar SOFC geometry. The model has been developed specifically to bridge the gap between detailed dimensional SOFC modeling and bulk SOFC models for use in whole-plant level IGFC system analysis. The current model thus has the following characteristics: (1) it is based upon detailed electrochemical analysis and internal heat transfer calculations; (2) it can give not only SOFC overall performance but also internal profiles of temperature, current density, flow compositions, etc., so that detailed SOFC operating conditions under different system configurations can be investigated; (3) it is computationally efficient and robust; and (4) it contains the flexibility to be directly linked to system analysis tools (such as chemical flow sheet software Aspen Plus® [19]). Special attention has been paid to making the model capable of reflecting some recent developments in SOFC technology, such as direct internal reforming (DIR), anode supported geometry, and the use of metallic interconnects. In addition, the electrochemical parameters of the model were determined through sensitivity analyses to match the SOFC performance observed by modern SOFC developers [14].

Table 1
SOFC cell single channel geometric parameters (co-flow or counter-flow).

Flow channel length	300 mm
Flow channel width (both fuel and air)	3 mm
Fuel channel height	1 mm
Air channel height	2 mm
Anode thickness	1 mm
Cathode thickness	0.05 mm
Electrolyte thickness	0.01 mm
Interconnect thickness	3.5 mm
Rib width	2.42 mm

The model is capable of simulating the two parallel-flow configurations (co-flow and counter-flow), which are believed to be sufficiently representative for the purposes of system analysis. The structures of fuel flow channel, air flow channel, positive electrode–electrolyte–negative electrode (PEN) structure, and air- and fuel-side interconnects (including rib structures) are resolved. The geometric configuration of the model is shown in Fig. 1. The anode-supported configuration that minimizes ohmic losses through use of a very thin electrolyte is commonly used in modern planar SOFC. Recently, SOFC producers have also reported successful fabrication of cells of large area up to 1000 cm^2 (33 cm × 33 cm) [20]. Throughout this work, a set of geometric parameters that can well represent such a trend of planar SOFC size and performance has been employed and the parameters that define this geometry are listed in Table 1.

The fuel cell model consists of two interacting modules: the "species conservation" (SC) module and the "energy conservation" (EC) module. The SC module accounts for detailed electrochemical and chemical reactions to calculate the species profiles and current density distribution within the SOFC. It is assumed that only H_2 participates in electrochemical reactions, while CO is oxidized through the water gas shift reaction. CH_4 is converted into CO and H_2 through the internal steam reformation reaction, which is kinetically limited. Side reactions such as direct electrochemical oxidation of CO, or dry reforming of CH_4, are assumed to be of little effect and are not included in the calculations. The EC module calculates temperature distribution, heat transfer, and heat loss throughout the fuel cell. Data are transferred between the two modules iteratively until the calculation convergence criteria are satisfied. Some important equations and parameters employed in the SC module are summarized in Table 2. Some energy conservations (for co-flow case) employed in the EC module are summarized in Table 3; by linearizing the species' specific enthalpies, the energy equations in the EC module are written into tridiagonal matrices, which can be solved very efficiently by the tridiagonal matrix algorithm (TDMA) [21].

More detailed features of the model and typical modeling results when running the model as a stand-alone analysis tool were presented in a previous paper [14]. In addition, the model has demonstrated that except for the very simple case of hydrogen fuel with co-flow configuration, SOFC operation generally results in complicated internal temperature, species, and current density profiles that should be resolved in systems analyses.

This work focuses upon the additional insights provided by this dimensional model (compared to a non-dimensional SOFC model) in an IGFC system analysis work and the changes in system design that must be considered due to the insights produced by the dimensional model. To achieve this goal, the developed SOFC model was programmed in FORTRAN language and linked with the Aspen Plus® process engineering flow sheet software package. A user-defined linking interface (also programmed in FORTRAN) is set up

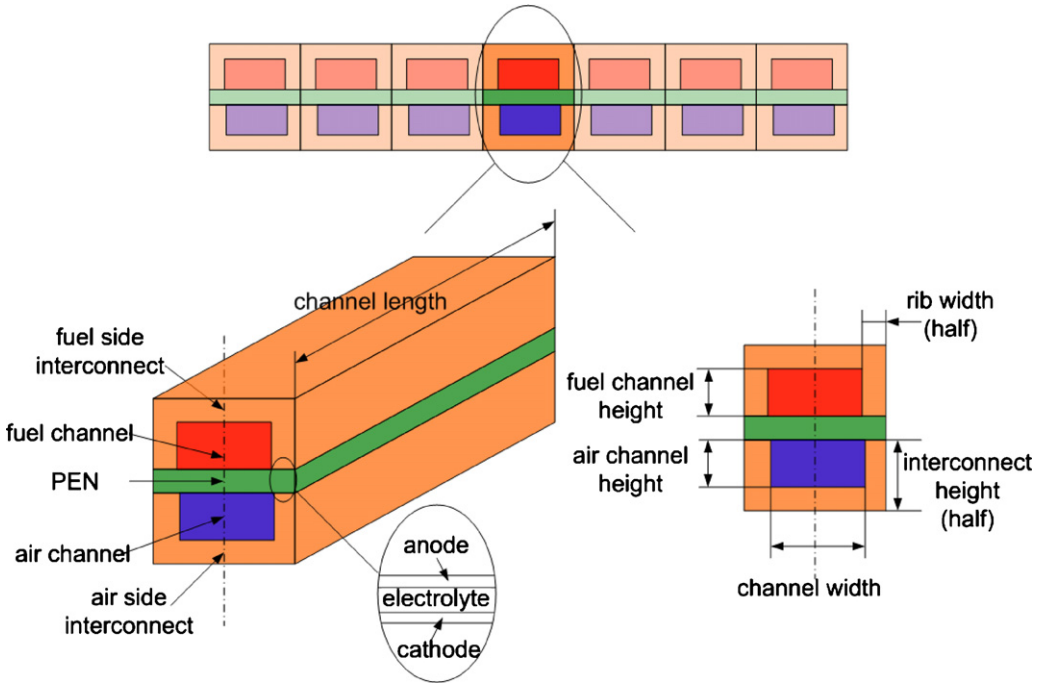

Fig. 1. Fuel cell geometry for co- and counter-flow planar SOFC (cited from [14]).

Table 2
Summary of major equations and parameters employed in the SOFC species conservation module.

Electrochemical sub-model: $V_{cell} = V_{Nernst} - \eta_{act} - \eta_{ohm} - \eta_{dif} = f(j)$	
Nernst potential [22]	$V_{Nernst} = E^0 + \frac{R_u T_{PEN}}{2F}\left[\ln\left(\frac{x^b_{H_2}(x^b_{O_2})^{1/2}}{x^b_{H_2O}}\right) + 0.5\ln\left(\frac{p_{cat}}{p_{amb}}\right)\right]$ where: $E^0 = 1.28628053 - 2.8873\times10^{-4}T_{PEN}$
Activation polarization [23]	$\eta_{act} = \frac{R_u T_{PEN}}{\alpha n F}\sinh^{-1}\left(\frac{j}{2j_0}\right)$
Anode side exchange current density $j_{0,an}$ [14,24,25] [a]	$j_{0,an} = \gamma_{an}\left(\frac{pH_2}{p_{amb}}\right)\left(\frac{pH_2O}{p_{amb}}\right)\exp\left(-\frac{E_{act,an}}{R_u T_{PEN}}\right)$ where: $\gamma_{an} = 5.5\times10^8$ A m^{-2} ; $E_{act,an} = 50$ kJ mol^{-1}
Cathode side exchange current density, $j_{0,cat}$ [14,24,25] [a]	$j_{0,cat} = \gamma cat\left(\frac{p_{O_2}}{p_{amb}}\right)^{0.25}\exp\left(-\frac{E_{act,cat}}{R_u T_{PEN}}\right)$ where: $\gamma_{cat} = 7\times10^8$ A m^{-2} ; $E_{act,cat} = 100$ kJ mol^{-1}
Ohmic polarization	$\eta_{ohm} = i(R_{PEN} + R_{IC,fuel} + R_{IC,air})$
	$\eta_{dif} = \eta^{an}_{dif} + \eta^{cat}_{dif} = \frac{R_u T_{PEN}}{2F}\ln\left(\frac{x^b_{H_2}x^r_{H_2O}}{x^b_{H_2O}x^r_{H_2}}\right) + \frac{R_u T_{PEN}}{4F}\ln\left(\frac{x^b_{O_2}}{x^r_{O_2}}\right)$
Diffusion polarization [26]	where : $x^r_{H_2} = x^b_{H_2} - \frac{jR_u T_{PEN}\delta_{an}}{2Fp_{an}D_{an,eff}}$
	$x^r_{H_2O} = x^b_{H_2O} + \frac{jR_u T_{PEN}\delta_{an}}{2Fp_{an}D_{an,eff}}$
	$x^r_{O_2} = 1 + (x^b_{O_2} - 1)\exp\left(\frac{jR_u T_{PEN}\delta_{cat}}{4Fp_{cat}D_{cat,eff}}\right)$
Water gas shift reaction: $CO + H_2O = H_2 + CO_2$ Assumed to be always in local equilibrium [25]	$K_{p,shift} = \frac{p_{H_2}p_{CO_2}}{p_{H_2O}p_{CO}} = \frac{x_{H_2}x_{CO_2}}{x_{H_2O}x_{CO}} = \exp\left(\frac{4276}{T_{fuel}} - 3.961\right)$
Methane reformation: $CH_4 + H_2O \rightarrow 3H_2 + CO$ Kinetics controlled [27]	$r_{rx} = \gamma_{rx}p_{CH_4}\exp\left(-\frac{E_{act,rx}}{R_u T_{PEN}}\right)A_{rx}$
	where : $\gamma_{rx} = 4274$ mol s^{-1} m^{-2} bar^{-1}
	$E_{act,rx} = 82$ kJ mol^{-1}

[a] Parameters obtained through sensitivity analysis, see [14] for more details.

to transfer information between the SOFC model and the Aspen Plus® main program so that Aspen Plus® can call the dimensional SOFC model automatically in an iterative calculation process and thus eliminate the tedious labor and possible mistakes that might otherwise be involved in copying and transferring large amounts of data between different computer programs. Fig. 2 shows the representation of a quasi-two-dimensional co-flow SOFC model in Aspen Plus®, where the streams "FUEL", "OXID", "ANEX", and "CAEX" represent fuel inlet, oxidant inlet, anode exhaust and cathode exhaust, respectively; "FCWORK" is the electricity produced by the SOFC

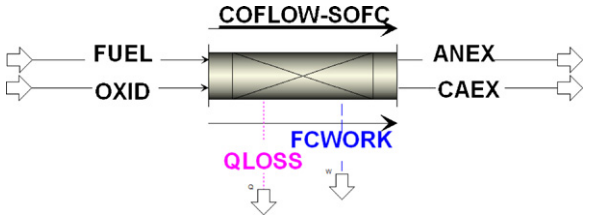

Fig. 2. Representation of a quasi-two-dimensional co-flow SOFC model in Aspen Plus®.

Table 3
Summary of major equations employed in the SOFC energy conservation module, co-flow case.

The ith control volume in the fuel channel	$\sum_k n_k(i)h_k(i-1) - \sum_k n_k(i+1)h_k(i) + K_{fuel}A_{fuel-PEN}(T_{PEN}(i) - T_{fuel}(i)) + K_{fuel}A_{fuel-IC}(T_{IC}(i) - T_{fuel}(i)) - r_{rx}(i)h_{CH_4}(i) - r_{rx}(i)h_{H_2O}(i) + r_{rx}(i)h'_{CO}(i) + 3r_{rx}(i)h'_{H_2}(i) - r_{ele}(i)h_{H_2}(i) + r_{ele}(i)h'_{H_2O}(i) = 0$ where: $k = H_2$, CH_4, CO, CO_2, H_2O, N_2 and Ar
The ith control volume in the air channel	$\sum_k n_k(i)h_k(i-1) - \sum_k n_k(i+1)h_k(i) + K_{air}A_{air-PEN}(T_{PEN}(i) - T_{air}(i)) + K_{air}A_{air-IC}(T_{IC}(i) - T_{air}(i)) - \frac{1}{2}r_{ele}(i)h_{O_2}(i) = 0$ where: $k = O_2$, N_2, CO_2, H_2O and Ar
The ith control volume in the PEN	$\frac{T_{PEN}(i-1)-T_{PEN}(i)}{R_{PEN}} + \frac{T_{PEN}(i+1)-T_{PEN}(i)}{R_{PEN}} + \frac{T_{IC}(i)-T_{PEN}(i)}{R_{PEN-IC}} + K_{fuel}A_{fuel-PEN}(T_{fuel}(i) - T_{PEN}(i)) + K_{air}A_{air-PEN}(T_{air}(i) - T_{PEN}(i)) - W_{ele}(i) + r_{rx}(i)h_{CH_4}(i) + r_{rx}(i)h_{H_2O}(i) - r_{rx}(i)h'_{CO}(i) - 3r_{rx}(i)h'_{H_2}(i) + r_{ele}(i)h_{H_2}(i) + \frac{1}{2}r_{ele}(i)h_{O_2}(i) - r_{ele}(i)h'_{H_2O}(i) = 0$
The ith control volume in the interconnect	$\frac{T_{IC}(i-1)-T_{IC}(i)}{R_{IC}} + \frac{T_{IC}(i+1)-T_{IC}(i)}{R_{IC}} + \frac{T_{PEN}(i)-T_{IC}(i)}{R_{PEN-IC}} + K_{fuel}A_{fuel-IC}(T_{fuel}(i) - T_{IC}(i)) + K_{air}A_{air-IC}(T_{air}(i) - T_{IC}(i)) = 0$

stack and "QLOSS" is the heat loss of the SOFC stack to the environment. SOFC model results that are essential for the system analysis to carry on (such as flow rates and thermodynamic properties of SOFC outlet streams) are transferred back to the Aspen Plus® program automatically, the rest of the results can either be returned to the Aspen Plus® program through the "User Arrays" form or saved in a separate formatted data output file.

3. The "baseline" case and performance

The "baseline" IGFC system employed in this work is the most promising design obtained in previous non-dimensional SOFC model based IGFC system design work [12]. The block flow diagram of the baseline system is shown in Fig. 3. The system consists of a catalytic hydro-gasification sub-system, proven low-temperature gas cleaning equipment, and a hybrid fuel cell – gas turbine power block (with the SOFC operating at about 10 bar). The system uniquely features recycling of the de-carbonized, humidified SOFC anode exhaust gas back to the hydro-gasifier for improved energy integration.

The catalytic hydro-gasifier [28] is capable of producing a syngas with high CH_4 content at high cold gas efficiency. The CH_4 content in the syngas can be internally reformed in the SOFC and the chemical cooling provided by this endothermic reaction can significantly reduce the flow rate of cooling air required by the SOFC, thus decreasing the parasitic load of SOFC stack air compression. This is a very important contributing element to the overall system efficiency of several recently proposed highly efficient IGFC systems [11,12].

The system is estimated to be able to achieve a thermal efficiency of 58.4% while capturing 94% of the carbon present in syngas as a compressed CO_2 stream. The efficiency achieved by this configuration can be as high as 61.5% if it is not required to compress the separated CO_2 stream to a high pressure. Detailed system performance data of the "baseline" case are listed in Table 4.

The non-dimensional SOFC model in the "baseline" case is replaced with the dimensional SOFC and the system performance is scrutinized in detail, as will be shown in the following sections.

4. IGFC system analysis using dimensional SOFC models

4.1. Non-dimensional SOFC model analysis: a recapitulation

In the "baseline" system, because the non-dimensional SOFC model cannot resolve the internal temperature and species distributions within SOFC stacks, the following SOFC performance characteristics have been employed or assumed:

1. It is assumed that the temperatures of the fuel and air flows are very close to those of the solid structures (PEN and the interconnect structure) everywhere inside the SOFC cell, thus the temperatures of the fuel and air flows are good approximations of the temperatures of the solid structures.
2. Fuel and air inlet temperatures are both 923 K (650 °C), this can be achieved by providing sufficient preheating to the inlet fuel and air flows.
3. It is assumed that fuel and air outlet temperatures are both 1123 K (850 °C).
4. A design criterion requires that SOFC maximum operation temperature does not exceed 1123 K (850 °C). With the 3rd assumption described above, it is implicitly assumed that the maximum temperature within SOFC channel occurs at the fuel and air outlet sides.
5. Another design criterion requires a maximum SOFC ΔT (difference between highest temperature and lowest SOFC temperature) that is no larger than 200 K. Combining the 2nd and 3rd assumptions described above, it can be seen that the maxi-

Table 4
Summary of thermal performance of the "baseline" IGFC plant.

Major gross power output (MW)	
SOFC electrical power	247.77
Cathode exhaust expander	63.38
Steam turbine	2.53
Reactor/expander topping cycle	9.34
Total gross power generated	323.26
Major auxiliary power consumption (MW)	
Coal milling and handling	0.60
Coal pump	1.60
ASU air compressor	1.55
ASU O_2 compressor	0.55
SOFC air compressor	66.91
Anode exhaust compressor	4.33
Recycled H_2 compressor	3.91
Selexol™ unit	0.98
MDEA unit	0.62
Cooling tower fan	0.45
Cooling tower pump	0.85
Condensate recycle pump	0.29
BFW feed pump	0.16
Transformer losses	0.70
CO2 compression	11.57
Miscellaneous BOP & lighting	1.00
Total internal power consumption and losses	96.50
Overall performance	
Net electric power (MW)	226.76
Carbon capture rate	93.7%
Overall thermal efficiency (% coal HHV)	58.4%

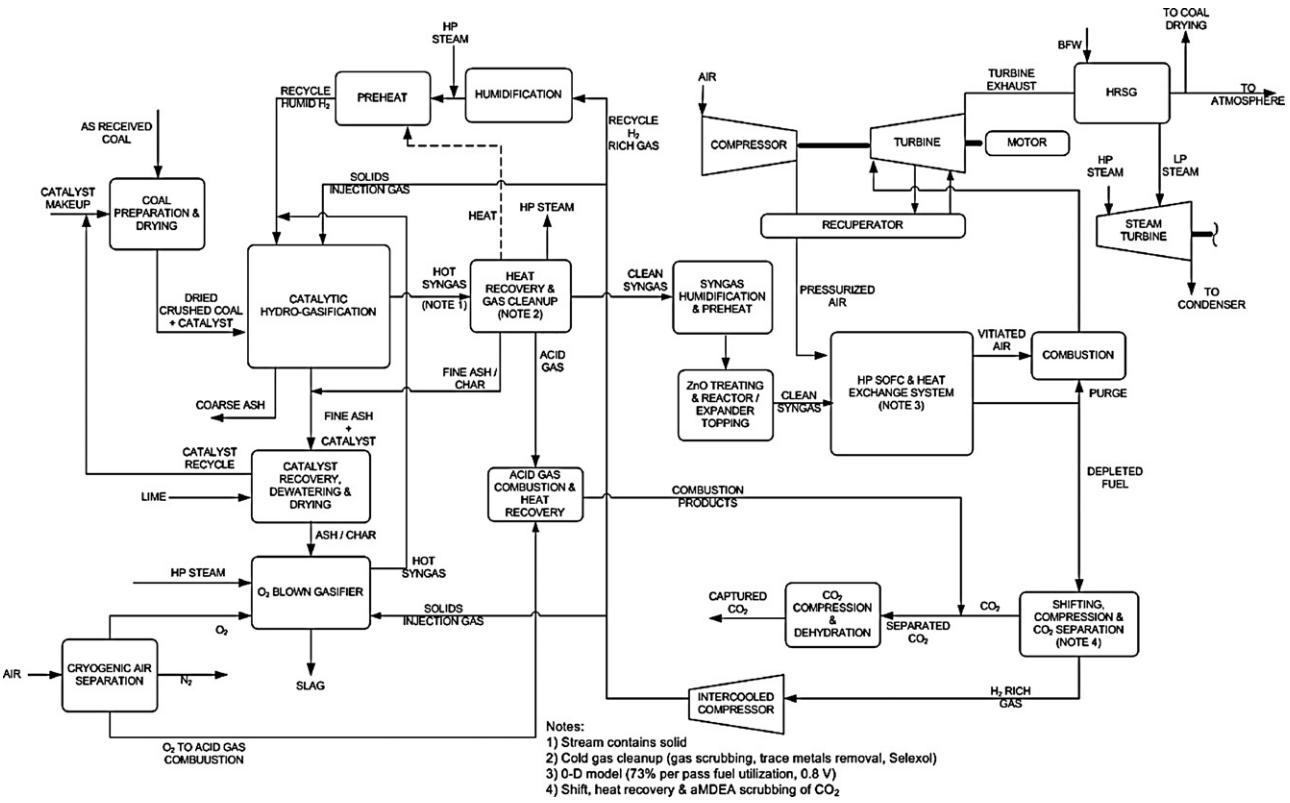

Fig. 3. Block flow diagram of "baseline" case: IGFC power only plant with pressurized SOFC and anode exhaust recycled to the gasifier.

mum ΔT is implicitly assumed to be the difference between the flow outlet temperature and inlet temperature.

6. The SOFC maximum air utilization factor is assumed to be 58%; this will approximately result in O_2 mole fraction of 10% in the cathode exhaust.

A non-dimensional SOFC model confirmed that these performance characteristics are thermodynamically correct and do not violate any mass or energy balance requirements. However, with the insights provided by the detailed dimensional SOFC models, it is found that some of the assumptions listed above turn out to be unrealistic or erroneous, i.e., impossible to achieve given the geometry, physics, chemistry and electrochemistry extant in an SOFC.

4.2. Insights provided by a dimensional SOFC model

SOFC with co-flow and counter-flow configurations in IGFC systems have been investigated using the dimensional SOFC model described above.

It is found that when the inlet fuel contains a significant amount of CH_4, co-flow operation becomes very challenging due to a severe temperature dip at the fuel and air inlet edge. In a co-flow configuration, at the fuel inlet edge the steam methane reforming is so strong that the cell temperature drops dramatically and the chemical and electrochemical reaction kinetics are all slowed down significantly. The cell ends up with very low fuel and air utilization as well as very poor current and power density. Fig. 4 shows a temperature dip in a co-flow configuration SOFC. The SOFC inlet fuel contains about 21.4% H_2, 4.0% CO, 10.5% CO_2, 30.9% H_2O and 27.6% CH_4 (molar fractions, balanced by N_2 and Ar); this fuel composition is typical in the IGFC cases discussed in this work.

In contrast, the counter-flow configuration has some advantages and is generally less susceptible to severe temperature dips at the fuel inlet side because the air flow has picked up enough heat in the cathode channels before reaching the air outlet edge (fuel inlet edge) and thus can provide enough heating for the endothermic steam methane reformation occurring at the location. It should be pointed out that the counter-flow configuration can still encounter temperature dips that are severe enough to hamper operation when the syngas contains very large amounts of CH_4 (more than 35 vol.% CH_4) and the air flow rate is pushed to a relatively low level.

Another point regarding SOFC operation on CH_4-rich syngas is that the counter-flow configuration generally has appreciably higher average current and power density than the co-flow configuration. This finding is because counter-flow SOFC with internal steam methane reforming can result in species and temperature distributions in which the area of high temperatures (correspond-

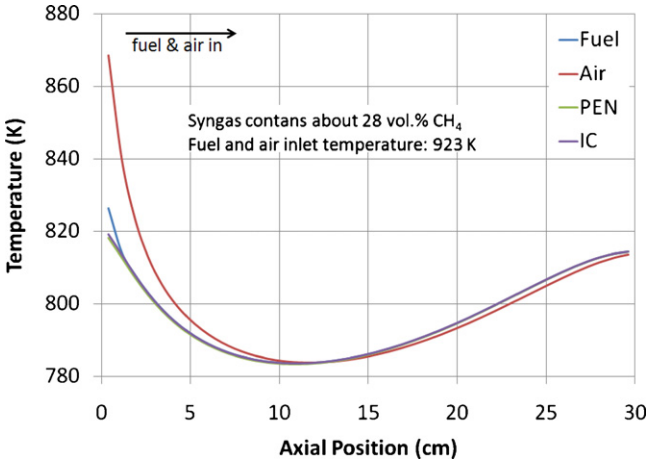

Fig. 4. Temperature dip in co-flow SOFC operating on CH_4 rich syngas.

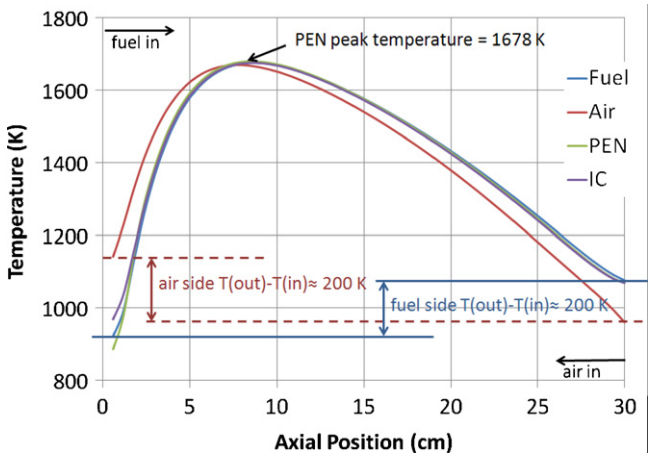

Fig. 5. "Correct" non-dimensional SOFC model operation conditions result in extremely high internal temperature spike in counter-flow SOFC.

ing to smaller polarization losses) and the area of high fuel/oxidant chemical potential difference (leading to higher Nernst potential) overlap each other in relatively larger portion of the cell (see [12] for more details and discussions on this topic).

In IGFC designs in which CH_4-rich syngas is produced to fully take advantage of the cooling effect of internal steam methane reforming (such as the "baseline" case in this work), the CH_4 content in the fuel to the SOFC can be 25 vol.% or even higher. Thus, the counter-flow configuration is a preferable choice in these cases and worth more detailed investigation.

The challenge associated with a counter-flow configuration, however, is the temperature spike that occurs within the SOFC. For example, using a quasi-two-dimensional counter-flow SOFC model, it is possible to find a working case with inlet and outlet flow conditions that closely match those working characteristics obtained from a non-dimensional SOFC model. Fig. 5 shows the internal temperature distributions of this case. It can be seen that the temperature rise from fuel inlet to outlet and air inlet to outlet are both approximately 200 K, which matches that predicted by a non-dimensional SOFC model; but the internal temperature peak in the PEN structure reaches almost 1700 K, which is obviously much higher than the safe operating temperature of a state-of-the-art SOFC. Thus, while thermodynamically correct operating conditions can be defined by a non-dimensional SOFC model, actual performance can be unacceptable due to cell internal temperature distributions, which can only be revealed by a dimensional SOFC model.

4.3. Required modification of the "baseline" system

Based on the observations described in Section 4.2, when putting the quasi-two-dimensional counter-flow SOFC model into the "baseline" case for a whole system analysis, the following design criteria must be added:

1. In the non-dimensional "baseline" design the air flow rate to the SOFC stack is varied to achieve about 50% air utilization. Now to mitigate an unacceptably high temperature spike in the SOFC, the air flow rate is varied so that the ΔT (defined as difference between highest temperature and lowest temperature) in PEN structure is within 200 K. In this case the actual air utilization is calculated in the SOFC model and reported by the SOFC model in the "User Arrays" form in Aspen Plus®. The temperature of the PEN structure is explicitly reported by the quasi-two-dimensional model; thus, it is no longer necessary to estimate the temperature of PEN based upon the temperatures of the fuel and air flows. It is implicitly assumed that the temperature of PEN is very close to that of the interconnect structure; this is justified by previous dimensional model results reported in [12].
2. The SOFC fuel utilization is determined by the H_2 requirement of the hydro-gasifier, which remains the same as in the "baseline" case. But because the SOFC geometry is now resolved, the desired fuel utilization must be achieved by varying the number of SOFC stacks, number of cells in each stack as well as number of channels in each cell.
3. The inlet fuel and air streams are still designed to be preheated to 923 K (650 °C), this design will help maintain a reasonable cell operating temperature level. Together with the 1st design criterion described above, this design also makes sure that the peak temperature in the SOFC does not exceed 1123 K (850 °C).
4. The SOFC stack chamber (containment vessel) temperature is varied so that the heat loss of the SOFC stacks is about 1% of the heat generated during chemical and electrochemical reactions.

The SOFC stack working voltage is set to be 0.8 V, which is consistent with state-of-the-art SOFC performance and is the same as the value assumed in the "baseline" case, for comparison.

The quasi-two-dimensional counter-flow SOFC model was plugged into the "baseline" case to replace the original non-dimensional SOFC model and a converged Aspen Plus® simulation was obtained, which is designated the "single stage counter-flow SOFC" case.

Before jumping to the discussion of overall thermal performance of the modified case, it is important to first observe the design changes that had to be made as a result of including the physics included in the dimensional SOFC model. Most of the original IGFC system components and operating designs of the "baseline" case remain unchanged; however, the important changes concern the methanation reactor in the reactor/expander topping cycle and the SOFC downstream pre-reformer: these two components were removed to deal with the much colder SOFC anode exhaust.

In the IGFC "baseline" design, because the pressure of the clean syngas is much higher than the operating pressure of the SOFC, it is preferable to put the syngas through a syngas expander to produce some useful work before sending it to the SOFC stack. A shift reactor and a methanation reactor can be placed before the expander to increase the syngas temperature (both the water–gas-shift reaction and the methanation reaction are exothermic) for higher overall efficiency. This system component is called a "reactor/expander topping cycle" [29] and has been demonstrated to be able to increase system thermal efficiency appreciably in IGCC systems. Because of the methanation reaction, the fuel coming out of the methanation reactor contains a large amount of CH_4 (as much as 36 vol.% CH_4). Under some operating conditions, the heat required to internally reform so much CH_4 is even larger than the overall heat released during the chemical and electrochemical reactions in the SOFC. Such a global energy imbalance around the SOFC stack can be well captured by the non-dimensional SOFC model (under similar conditions a dimensional SOFC model will end up with a serious temperature dip, which also indicates an impractical operating condition). Thus, for stable SOFC operation some of the CH_4 needs to be pre-reformed externally, this is achieved by splitting some of the syngas to an external pre-reformer with the remainder being sent to a pre-heater. The heat requirements of the pre-heater and the pre-reformer are both provided by the hot SOFC anode exhaust. The split ratio actually determines how much CH_4 is reserved for internal steam methane reforming and as heat sink within the SOFC stacks. In the "baseline" case a design specification is created in Aspen Plus® to automatically vary the split ratio to satisfy the heat balance requirement of the SOFC stack. The reactor/expander cycle design is schematically shown in Fig. 6. The benefit of this

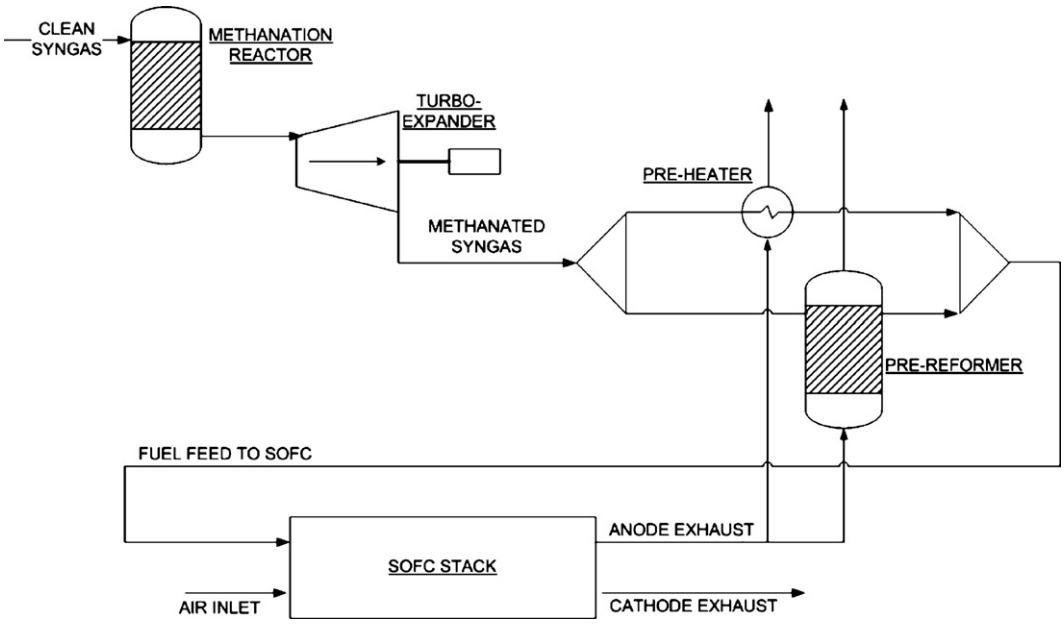

Fig. 6. Reactor/expander topping cycle, pre-reformer and pre-heater design in the "baseline" case.

design is that the sensible heat carried by the anode exhaust can be effectively recovered in the topping reactor/expander cycle to produce useful work and the system becomes more efficient. As described above, the fuel flow outlet temperature is assumed to be close to the maximum operating temperature of the SOFC in the non-dimensional SOFC model analysis and thus the anode exhaust is at high temperature which enables significant heat recovery.

On the other hand, when the quasi-two-dimensional SOFC model is included in the analysis it is found that the anode exhaust temperature is not as high as that predicted previously. The internal temperature profiles of the SOFC stack in this new working case are shown in Fig. 7. It can be seen that the anode exhaust temperature is about 943 K, which is only an increase of 20 K compared to the fuel inlet temperature (instead of 200 K). This small temperature rise would make it very challenging for heat transfer, requiring very large (and expensive) heat exchangers to the anode inlet stream. Moreover, the pre-reformer is more energy intensive than the pre-heater due to the endothermic steam methane reforming reaction and the anode exhaust predicted by the dimensional SOFC model no longer contains sufficient heat energy for this purpose; thus, the pre-reformer must be removed in the new design that employs the dimensional SOFC model. Correspondingly, the methanation reactor in the reactor/expander topping cycle also must be removed. Thus, some benefits associated with the reactor/expander topping cycle design must be forfeited when considering the physics of a dimensional SOFC model.

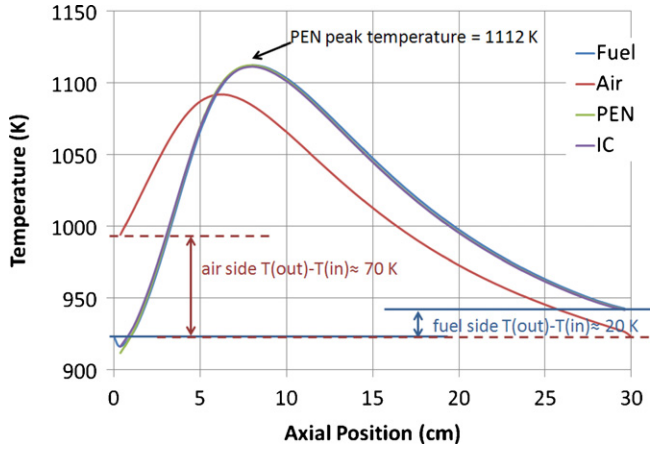

Fig. 7. Internal temperature distributions of SOFC in the "single stage counter-flow SOFC" IGFC design.

With these IGFC system differences in mind, we can now consider and discuss the thermal performance of the "single stage counter-flow SOFC" case. The major performance characteristics of this new case are compared with those of the "baseline" case in Table 5, along with the performance of other system configurations that will be discussed later in this paper. It can be seen that the system can only achieve a thermal efficiency of 42.1%, which is more than 15 percentage points lower than the result obtained from the non-dimensional SOFC model "baseline" case. This is mainly due to the huge parasitic load of the SOFC air compressor that is required to maintain the SOFC within the temperature constraints (not primarily due to system configuration differences discussed above). In Fig. 7 it can be seen that the SOFC internal peak temperature is well controlled to be lower than the maximum limit and this is achieved by increasing the cooling air flow rate significantly: the non-dimensional SOFC model predicted that the SOFC air utilization can be as high as 0.58, while in the quasi-two-dimensional SOFC model analysis the air flow rate has to be two and a half times larger to satisfy the cell ΔT and peak temperature requirements, resulting in a much smaller air utilization of only 0.16. It can be seen that the new system has a much larger gross power output thanks to the larger air flow rate to the cathode exhaust expander, but the increase in auxiliary power consumption is even more significant, and the net effect is a much lower net power output and lower overall system efficiency.

Thus, the application of a quasi-two-dimensional SOFC model has revealed more stringent requirements regarding the operation of SOFC stacks. To satisfy these requirements, particularly to satisfy the peak temperature and maximum ΔT requirements of the SOFC, many of the expected benefits associated with internal steam methane reforming are diminished, resulting in a system efficiency that is significantly lower than that previously predicted by non-dimensional SOFC model based analysis. The next section will investigate several SOFC module design options that may be used to still achieve high

Table 5
Summary and comparison of the thermal performance of IGFC systems (the "baseline" case uses the non-dimensional SOFC model, while all other cases use the dimensional SOFC model).

	Baseline	Single stage counterflow SOFC	Single stage counterflow SOFC (higher voltage)	Four stage air cascading counterflow SOFCs
SOFC performance parameters				
SOFC operation pressure (bar)	10.1	10.1	10.1	10.1
SOFC voltage (V)	0.8	0.8	0.85	0.8
SOFC single pass fuel utilization	0.73	0.72	0.73	0.73
SOFC single pass air utilization	0.58	0.16	0.19	0.46
Fuel outlet temperature (K)	1123	943	940	970
Air outlet temperature (K)	1123	994	986	1032
Major gross power output (>1 MW)				
SOFC electrical power	247.77	247.31	262.80	247.83
Cathode exhaust expander	63.38	178.60	146.08	72.10
Steam turbine	2.53	1.90	1.90	2.67
Reactor/expander topping cycle	9.34	7.58	7.58	7.21
Total gross power generated (MW)	323.26	435.62	418.59	330.41
Major auxiliary power consumption (>1 MW)				
Coal pump	1.60	1.60	1.60	1.60
ASU air compressor	1.55	1.55	1.55	1.55
SOFC air compressor	66.91	242.50	203.33	84.75
Anode exhaust compressor	4.33	4.34	4.34	5.88
Recycled H2 compressor	3.91	3.94	3.93	3.91
CO2 compression	11.57	11.63	11.63	11.63
Total internal power consumption and losses (MW)	96.50	272.14	232.92	115.96
Net electric power (MW)	226.76	163.49	185.67	214.45
Overall thermal efficiency (% coal HHV) 58.4%	42.1%	47.8%	55.2%	

IGFC system efficiency while meeting all of the SOFC design constraints.

5. Options for improving IGFC system performance, considering SOFC species and temperature distributions

5.1. Higher SOFC working voltage

A higher SOFC working voltage is desirable because: (1) higher working voltage makes the SOFC stack more efficient; (2) a larger portion of the chemical energy in the fuel is converted into electric power and less is released as heat. Thus, increasing SOFC operating voltage may help mitigate the extreme temperature spike and reduce the required cooling air flow rate and the associated compression power. While this design change could benefit and could have been anticipated with a non-dimensional model, the significant need for this change could not have been revealed without the dimensional SOFC model.

With the progress of SOFC performance reported in the recent years and the expectation that SOFC performance will continue to improve, a high working voltage of 0.87 V has been assumed in the DOE IGFC report analysis work [11]. In the "baseline" IGFC case, a relatively conservative working voltage of 0.8 V has been employed because with a non-dimensional SOFC model it is impossible to determine whether or not the SOFC can maintain a high working voltage due to either increased polarization losses or reduced Nernst potential at any point within the cell. With the help of a detailed quasi-two-dimensional SOFC model, it is now possible to investigate the performance of an IGFC system with higher SOFC working voltage while considering all of these constraints.

The "single stage counter-flow SOFC" IGFC case was modified and the cell working voltage was increased from 0.8 V to 0.85 V, the system thermal performance is reported in Table 5 along with that of the "baseline" case and the "single stage counter-flow SOFC" case.

The system thermal efficiency improves appreciably from 42.1% to 47.8%, thanks to: (1) relatively higher power output of the SOFC

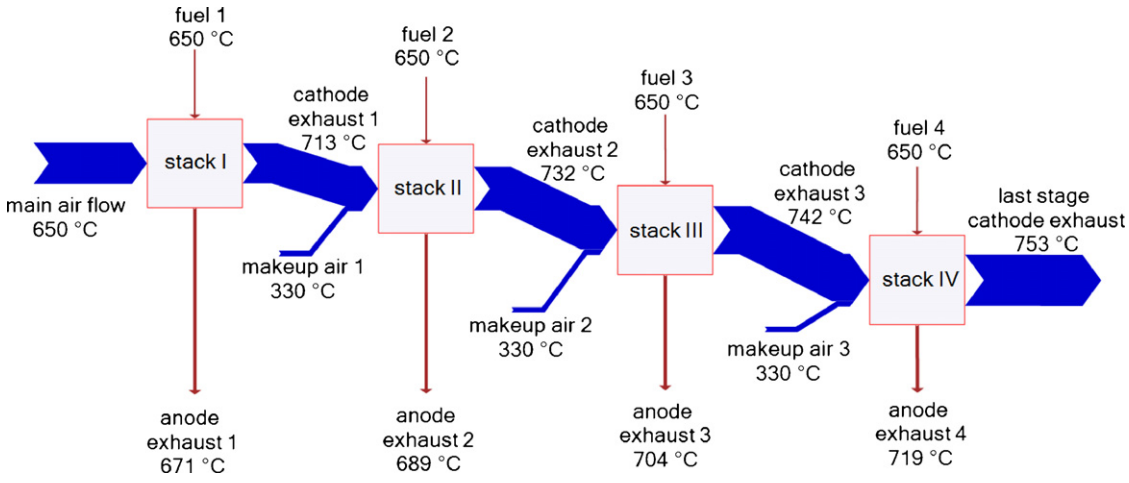

Fig. 8. Sankey diagram of the SOFC module design with four stages of cascading SOFC stacks.

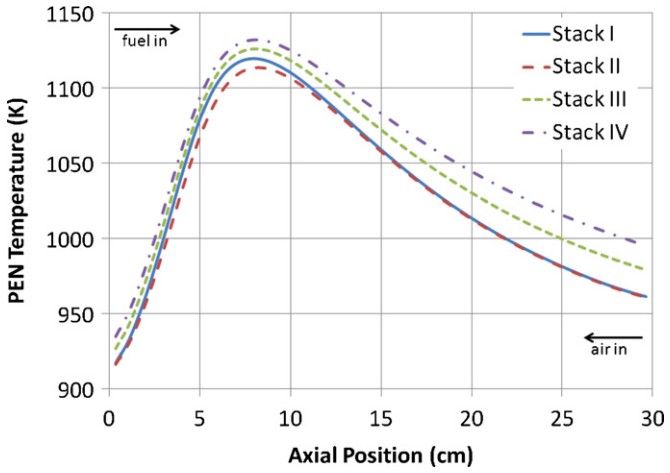

Fig. 9. Plot of PEN temperature distributions in the four cascading SOFC stacks.

stack, and (2) relatively smaller parasitic power consumption of the SOFC air compressor.

However, to satisfy the SOFC internal temperature requirements, a large amount of cooling air is still needed and the SOFC air utilization is only 0.19; this is why the system thermal efficiency is still significantly lower than that predicted in the "baseline" case. Besides, a drawback is that when SOFC working voltage is increased, the anode exhaust temperature becomes lower; this makes it more challenging to pre-heat the fuel stream with the anode exhaust.

It should be noted that increasing SOFC working voltage generally results in smaller average current density and for a prescribed total power output more SOFC stacks (and higher capital cost) will be needed. Thus, to determine an optimized cell working voltage one also needs to take into account economic factors, but this is beyond the scope of the current work. Also, it should be noted that due to the theoretical limit of Nernst potential, there is not much space to further increase the SOFC working voltage. Thus, although increasing cell working voltage can indeed improve IGFC system performance, raising the voltage alone cannot achieve IGFC system efficiency as high as that predicted by the non-dimensional SOFC model "baseline" case, while considering the constraints addressed by the dimensional SOFC model.

5.2. Cascading of identical SOFC stacks: a viable design strategy

Based upon the analysis work described above, it can be seen that a key factor for achieving high thermal efficiency is to reduce the overall cooling air flow rate (increase air utilization) while satisfying the SOFC stack safe operating temperature requirements.

An SOFC module design strategy is developed herein that is comprised of cascading identical SOFC stacks with series air flow, parallel fuel flow, and intra-stack introduction of fresh air to produce roughly identical operating conditions for each stack in the module. This design may be able to achieve high IGFC system efficiency because: (1) air utilization in each stack can be held low enough to effectively control the internal SOFC temperature peak; (2) the cathode exhaust coming out of one SOFC stack still contains large amount of O_2, which can be used in downstream stacks; (3) typically for the counter-flow configuration the cathode exhaust temperature is not significantly higher than the air inlet temperature, which assures that the cathode exhaust coming from upstream SOFC can still effectively work as a cooling flow in downstream SOFC stacks. Plus, fresh makeup air can be added in after each stack to provide more O_2, to cool the air flow to the desired temperature, and to provide roughly identical operating conditions for each stack. This design feature of the developed SOFC stack module concept is important to the cost of the system, which will depend upon the mass manufacturing of identical stack modules.

With the dimensional SOFC model successfully linked with Aspen Plus®, it is relatively easy to investigate various SOFC module configurations and parameters. A working design to be presented in the following section is comprised of four stages of cascading SOFC stacks. The SOFC sub-system design is shown in Fig. 8, with the plot representing a Sankey diagram [30] where the width of the streams represents the mass flow rate of each stream. The working voltage of each of the four staged SOFC stacks is set to 0.8 V. The total incoming fuel flow is pre-heated to 923 K (650 °C) and distributed evenly to the four SOFC stacks. The air flow is cascaded in series through the four stages of SOFC stacks, the main air flow fed to the first stage SOFC is also pre-heated to 923 K (650 °C). Small amounts of cold fresh makeup air are mixed with the cathode exhausts from stages I, II and III, to cool down the main air flow slightly as well as to provide more O_2 for electrochemical reaction in downstream stages. There is no need to pre-heat the makeup air because relatively lower temperature is desired for cooling purposes; thus makeup air coming out of the air compressor at about 603 K (330 °C) can be directly used. In the Aspen Plus® simulation, a design specification is set up to automatically vary the main air flow rate so that the ΔT in SOFC stack I (the first stage SOFC stack) does not exceed 200 K; three more design specifications are used to automatically vary the three makeup air flow rates so that the ΔT in stacks II, III, and IV are also no larger than 200 K.

The internal PEN temperature distributions of the four SOFC stages are plotted in Fig. 9, it can be confirmed that the PEN temperatures of all four stages of SOFC stacks are well controlled. More detailed performance results for the four SOFC stacks are summarized in Table 6.

It should be noted that the design parameters (geometry, cell properties, etc.) of each of the four stacks have been kept the same (i.e., all SOFC stacks in this cascaded stack design are identical) and the resulting thermal profiles within the four stacks are quite similar to each other. This will ensure that the same exact SOFC stacks can be used interchangeably amongst the four stages in this design and manufacturing of a repeat SOFC stack unit will help reduce the cost of the SOFC sub-systems.

Table 6
Performance of the cascading SOFC stacks.

	Stack I	Stack II	Stack III	Stack IV	Four stages
Working voltage (V)	0.8	0.8	0.8	0.8	0.8
Single pass fuel utilization	0.69	0.72	0.74	0.75	0.73 (overall)
Single pass air utilization	0.15	0.16	0.17	0.18	0.46 (overall)
Fuel inlet temperature (K)	923	923	923	923	923
Air inlet temperature (K)	923	942	961	979	N.A.
Fuel outlet temperature (K)	944	962	977	992	970 (anode exhausts mixture)
Air outlet temperature (K)	986	1005	1015	1026	1026 (last stage)
Maximum PEN temperature (K)	1103	1113	1126	1132	N.A.
Minimum PEN temperature (K)	907	916	927	935	N.A.
ΔT in PEN (K)	196	197	199	197	N.A.

The thermal performance of the whole IGFC system with the cascading SOFC stacks module design is presented in the last column of Table 5, along with the performance of the three other cases for comparison. By employing the cascading SOFC module design, the overall air utilization of the SOFC stacks can be increased to as high as 0.46; this is much closer to the "ideal" prediction made in the "baseline" case with a non-dimensional SOFC module. The parasitic power consumption of the SOFC air compressor also drops significantly, thanks to the much smaller overall cooling air flow rate. The system manages to achieve a thermal efficiency of 55.2%, which is only about 3 percentage points lower than that predicted using the non-dimensional model in the baseline case. This overall IGFC system efficiency is very impressive considering all the stringent temperature control requirements that have been imposed, and is especially promising in comparison to other strategies for electricity production from coal [31]. Besides, the last stage cathode exhaust temperature and the anode exhaust mixture temperature are both significantly higher than those achieved in the single stage SOFC cases, which is beneficial to the IGFC system design and operation of the pre-heaters.

A down side of the design is that some pressure head of the compressed flows is wasted because of the cascading stages, which is also part of the reason why the system overall efficiency is still lower than that predicted in the non-dimensional baseline case.

Overall the performance of the IGFC with cascading SOFC stacks is considered satisfactory and is the most promising system identified thus far.

6. Summary and conclusions

This work investigates the application of a detailed dimensional planar SOFC model in the design and analysis of coal-based IGFC systems. A detailed quasi-two-dimensional finite volume SOFC model [14] has been linked with Aspen Plus® to perform the analyses. The most promising case identified in previous non-dimensional SOFC model based design and analysis work [12] has been used as a starting point and "baseline" case.

Two major differences are observed when the dimensional SOFC model is used in place of the original non-dimensional SOFC model: (1) the anode/cathode exhaust temperatures end up much lower than those predicted using the non-dimensional SOFC model, which makes the heat transfer in the pre-heaters more challenging and renders the methanation reactor and external pre-reformer in the original "baseline" design no longer useful; (2) the cooling air flow rate required to control the internal temperature spike and ΔT is much larger than that predicted by the non-dimensional model, which significantly increases the parasitic power consumption of SOFC air compressor and seriously diminishes the system thermal efficiency. The modified system that only considers the additional constraints imposed by the dimensional SOFC model has an efficiency of 42.1%, which is disappointingly low for the novel IGFC system (even though it is still much higher than comparable IGCC cycles).

Design changes to improve the overall IGFC system efficiency while fully accounting for the SOFC operating constraints using the dimensional model have also been investigated. By increasing the SOFC working voltage from 0.8 V to 0.85 V, the IGFC system thermal efficiency increases from 42.1% to 47.8%, this is an impressive improvement but the system performance is still significantly lower than that predicted by the non-dimensional SOFC model. A design where air flow is cascaded in series through four stages of SOFC stacks is found to be quite an effective solution. In this design, multiple stages of identical SOFC stacks are employed, with parallel fuel flow and series air flow (with some fresh makeup air added after each stage). The design can achieve low air utilization (sufficient cooling) within each stage while maintaining relatively high overall air utilization. An SOFC sub-system comprised of four-stage cascading stacks can achieve an overall IGFC system efficiency of 55.2%, which is much closer to the "ideal" performance (58.4%) predicted using the non-dimensional SOFC model.

This work clearly demonstrates the advantages and importance of using detailed dimensional SOFC models to avoid over-simplified or even erroneous SOFC operating assumptions in IGFC systems analyses. Future work will explore the application of the dimensional SOFC model in other IGFC system configurations, such as cases with H_2 co-production or those that use oxygen-blown gasification, in which detailed and accurate knowledge of the SOFC stacks is also essential to the design work.

References

[1] D. Jansen, A.B.J. Oudhuis, H.M. van Veen, Energy Conversion and Management 33 (1992) 365–372.
[2] D. Jansen, P.C. van der Laag, A.B.J. Oudhuis, J.S. Ribberink, Journal of Power Sources 49 (1994) 151–165.
[3] M. Maruyama, S. Takahashi, J. Iritani, H. Miki, Status of the EAGLE Project: Coal Gas Production Technology Acceptable for Fuel Cells, 2000 Gasification Technologies Conference, San Francisco, CA, 2000.
[4] K.V. Lobachyov, H.J. Richter, Energy Conversion and Management 38 (1997) 1693–1699.
[5] T. Kivisaari, P. Björnbom, C. Sylwan, B. Jacquinot, D. Jansen, A. de Groot, Chemical Engineering Journal 100 (2004) 167–180.
[6] P. Kuchonthara, S. Bhattacharya, A. Tsutsumi, Fuel 84 (2005) 1019–1021.
[7] S. Ghosh, S. De, Energy 31 (2006) 345–363.
[8] S. Ghosh, S. De, International Journal of Energy research 30 (2006) 647–658.
[9] A.D. Rao, A. Verma, G.S. Samuelsen, Engineering and Economic Analyses of a Coal-fueled Solid Oxide Fuel Cell Hybrid Power Plant, GT2005-68762, ASME Turbo Expo 2005: Power for Land, Sea and Air, Reno-Tahoe, NV, 2005.
[10] A. Verma, A.D. Rao, G.S. Samuelsen, Journal of Power Sources 158 (2006) 417–427.
[11] K. Gerdes, E. Grol, D. Kearins, R. Newby, Integrated Gasification Fuel Cell Performance and Cost Assessment, DOE/NETL-2009/1361, U.S. Department of Energy, Morgantown, WV, 2009.
[12] M. Li, A.D. Rao, J. Brouwer, G.S. Samuelsen, Journal of Power Sources 195 (2010) 5707–5718.
[13] S.M. Klara, Advancing Coal Energy Technologies: Department of Energy R&D Program, 10th Annual SECA Workshop, Pittsburgh, PA, 2009.
[14] M. Li, J.D. Powers, J. Brouwer, Journal of Fuel Cell Science and Technology 7 (2010) 041017.
[15] R. Bove, S. Ubertini, Modeling Solid Oxide Fuel Cells: Methods, Procedures and Techniques, Springer, Berlin, Germany, 2008.
[16] C.Y. Wang, Chemical Reviews 104 (2004) 4727–4766.
[17] L. Ma, D.B. Ingham, M. Pourkashanian, E. Carcadea, Journal of Fuel Cell Science and Technology 2 (2005) 246–257.
[18] S. Kakaç, A. Pramuanjaroenkij, X.Y. Zhou, International Journal of Hydrogen Energy 32 (2007) 761–786.
[19] Aspen Plus, Aspen Plus User Guide, Aspen Technology Inc., Cambridge, MA, 2003.
[20] H. Ghezel-Ayagh, B. Borglum, Coal-Based SECA Program-Fuel Cell Energy Inc., 11th Annual SECA Workshop, Pittsburgh, PA, 2010.
[21] S. Patankar, Numerical Heat Transfer and Fluid Flow, 1st ed., Hemisphere, Washington, DC, 1980.
[22] J. Larminie, A. Dicks, Fuel Cell Systems Explained, 2nd ed., Wiley, West Sussex, England, 2003.
[23] D.A. Noren, M.A. Hoffman, Journal of Power Sources 152 (2005) 175–181.
[24] P. Costamagna, A. Selimovic, M.D. Borghi, G. Agnew, Chemical Engineering Journal 102 (2004) 61–69.
[25] S. Campanari, P. Iora, Journal of Power Sources 132 (2004) 113–126.
[26] S.H. Chan, Z.T. Xia, Journal of the Electrochemical Society 148 (2001) A388–A394.
[27] E. Achenbach, Journal of Power Sources 49 (1994) 333–348.
[28] T. Kalina, N.C. Nahas, Exxon Catalytic Coal Gasification Process Predevelopment Program Final Project Report, Exxon Research and Engineering Company, Bayton, TX, 1978.
[29] A.D. Rao, Reactor Expander Topping Cycle, U.S. Patent No. 4,999,993, March 1991.
[30] M. Schmidt, Journal of Industrial Ecology 12 (2008) 82–94.
[31] M.C. Woods, et al. (Eds.), Cost and Performance Baseline for Fossil Energy Plants, DOE/NETL-2007/1281, U.S. Department of Energy, Morgantown, WV, 2007.